A Sequential and Asynchronous Federated Learning Framework for Railway Point Machine Fault Diagnosis With Imperfect Data Transmission

Tao Wen, Xiaohan Chen, Dingcheng Zhang, Clive Roberts, *Member, IEEE*, and Baigen Cai, *Senior Member, IEEE*

***Abstract*—Fault diagnosis of railway assets has drawn the interest of both the scholarly and engineering communities. Federated learning (FL) enables training models across distributed assets to preserve data privacy and reduce high data transfer costs, which has been applied in fault diagnosis. However, the imperfect data transmission problem due to communication errors easily results in low accuracy of FL-based fault diagnosis in the railway system. To solve the problem, a sequential and asynchronous federated learning framework is proposed for fault diagnosis of railway point machines (RPMs) in this work. First, a dual-branch network is proposed as the global model in asynchronous FL for reducing parameters, while maintaining high accuracy. Second, a time cycle mechanism based on sequential Kalman filtering is proposed for reducing the negative impact of data communication errors. Finally, experimental results demonstrates that the proposed method enhances the applicability of online RPM fault diagnosis training in real deployment scenarios.**

***Index Terms*—Communication error, deep learning, fault diagnosis, federated learning (FL), railway point machine (RPM), sequential Kalman filtering (SKF).**

Manuscript received 12 November 2023; revised 20 February 2024; accepted 1 March 2024. Date of publication 29 March 2024; date of current version 5 June 2024. This work was supported in part by the National Natural Science Foundation of China under Grant 62120106011, Grant 52172323, Grant 62027809, Grant 62273202, and Grant 52105115, and in part by the Sichuan Science and Technology Program under Grant 2023NSFSC0862. Paper no. TII-23-4491. *(Corresponding author: Dingcheng Zhang.)*

Tao Wen, Xiaohan Chen, and Baigen Cai are with the School of Automation and Intelligence, Beijing Jiaotong University, Beijing 100044, China (e-mail: wentao@bjtu.edu.cn; 22120218@bjtu.edu.cn; bgcai@bjtu.edu.cn).

Dingcheng Zhang is with the School of Mechanical Engineering, Sichuan University, Chengdu 610017, China (e-mail: dc_zhang@scu.edu.cn).

Clive Roberts is with the Birmingham Centre for Railway Research and Education, University of Birmingham, B15 2TT Birmingham, U.K. (e-mail: c.roberts.20@bham.ac.uk).

Color versions of one or more figures in this article are available at https://doi.org/10.1109/TII.2024.3378800.

Digital Object Identifier 10.1109/TII.2024.3378800

I. Introduction

RAILWAY transportation routes are expanding as the economy grows and the movement of people increases [1], [2]. Ensuring the safety of railway operations has drawn significant attention from both the industry and the academic community [3], [4]. Railway point machines (RPMs) as one of key assets are responsible for executing the switching process and determining the designated path of the train [5]. RPMs operate in open-air environments, subjecting them to diverse weather patterns, temperature fluctuations, and humidity levels, thereby rendering them vulnerable to various failures [6]. This can lead to economic losses and casualties. Fault diagnosis for RPMs enables to detect their early faults and avoid tragedies [7].

The vibration-based fault diagnosis methods have been widely employed to assess the operational state of mechanical systems. Researchers have put forward diagnosis methods based on vibration sensors for gearboxes [8], rotating machinery [9], and bearings [10]. The main fault type in RPMs is mechanical failure, and hence some vibration-based methods have been proposed for RPM fault diagnosis [11]. For instance, variational mode decomposition [12], wavelet transform [13] were applied to fault diagnosis of RPMs by extracting features. Above signal processing algorithms have achieved good performance in some cases. However, those methods rely on prior knowledge and experts' experience, which is characterized by low efficiency, limited timeliness, and elevated labor costs. To overcome problems, researchers proposed data driven methods for RPM fault diagnosis [11]. For example, a double-scale wide first-layer kernel convolutional neural network was proposed for fault diagnosis of ZDJ9 RPMs using low-sampling-rate vibration sensors [14]. A deep random forest fusion method was proposed to fuse the three-axis vibration signals of the RPM [15]. The data-driven RPM fault diagnosis methods exhibit a high level of accuracy and efficiency in above cases. However, it centralizes data resources from several RPMs onto a cloud server for training a fault diagnosis model by using the existing data driven methods. Those traditional centralized learning methods have limitations in real operation condition due to data security and commercial competition [16].

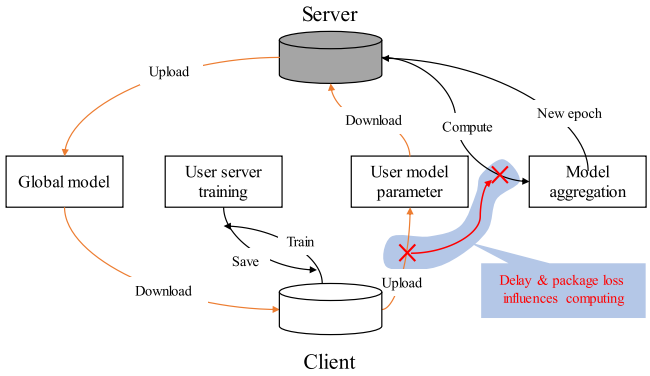

Fig. 1. Flowchart of synchronous FL with data delay and package loss.

Federated learning (FL) as one machine learning approach enables training models across decentralized and distributed devices or systems while keeping data localized and not centrally aggregated [17]. It offers a way to harness the collective intelligence of a network of devices while respecting data security and reducing data transmission [18]. FL has been used in various applications, including human activity recognition on smartphones [19], healthcare research [20], and object detection in IoT networks [21], [22]. Researchers have also applied FL for fault diagnosis. For example, a deep learning-based FL method with a dynamic validation scheme was proposed for rotating machinery fault diagnosis [23]. A class-imbalanced privacy-preserving FL framework was proposed for the fault diagnosis of a decentralized wind turbine, in which a biometric authentication technique was employed to protect private data and defend against malicious attacks [24]. An FL method was proposed for fault diagnosis of multirailway high-speed train bogies by using SecureBoost in the local diagnosis models [25]. Those methods based on synchronous FL have obtained good performance in cases.

In synchronous FL frameworks, the server however has to spend a considerable amount of time waiting for all data packets to arrive before performing aggregation computations, when data delays and packet losses occur as shown in Fig. 1. This results in high computational costs and reduced accuracy.

An fault diagnosis method based on asynchronous FL was proposed to obtain the optimal performance of the client by real-time updating the clients' network parameters [26]. This method takes into account the different order in which data arrives at the server due to time delays, but does not consider the case of data packet loss. Locations of railway assets are dispersed and there is a considerable distance between devices. Normally, real-time operational data of railway assets is transmitted wirelessly to a central server. Hence, the problem of imperfect data transmission, i.e., data delay and package loss, leading to inaccuracies and inefficiencies of FL-based fault diagnosis methods.

To solve the above problem, a sequential and asynchronous federated learning (SAFL) is proposed for fault diagnosis of RPMs. In the proposed method, a double-scale fully convolutional neural network (DS-FCN) is proposed to build the global model of the FL framework. In DS-FCN, the dual-branch architecture is constructed to extract features at different scales. Also, a time cycle mechanism based on sequential Kalman filtering (SKF) is proposed to fuse model parameters which are regularly distributed to all clients. The SKF-based aggregation algorithm of the federal center effectively mitigates potential communication errors. The key contributions of our research are summarized as follows.

1) A SAFL framework is proposed for RPM fault diagnosis considering conditions of imperfect data transmission in this work, which is the first research on FL in the field of RPM fault diagnosis.
2) To reduce the possibility of congestion and package loss in the data transmission, a double scale fully convolutional neural network is proposed to achieve comparable accuracy to existing methods while using fewer trainable parameters. This makes it highly suitable for parameter transfer in FL.
3) To remove the prolonged waiting period and obtain the accurate global fusion, a time cycle mechanism based on SKF is proposed to calculate sequential Kalman gain dynamically for estimating parameters when information delay and data package loss occur.

The rest of this article is organized as follows. Section II formulates the problem and the assumptions. In Section III, we put out our proposed framework, including the double scale fully convolutional neural network, asynchronous federated network, time cycle-based SAFL, and SAFL framework-based fault diagnosis for RPMs. We provided a detailed introduction to the operating process of ZDJ9 and sensor data for various working conditions in Section IV. We present detailed information on our experimental settings, evaluation metrics, results, and analysis and explanations in Section V. Finally, Section VI concludes this article.

II. Problem Formulation

In fault diagnosis methods based on FL frameworks, the server utilizes knowledge obtained from various clients to train a global model. The knowledge acquired by the global model is then fed back to the client models, reducing the need for direct transmission of client datasets. This work is conducted under three assumptions.

1) *Insufficient individual device data:* The data available on each individual device is not enough to train a robust and high-quality fault diagnosis model.
2) *Sample-partitioned FL:* All client devices have the same task categories, enabling collaborative training across clients and achieving horizontal federated learning.
3) *No sharing of data:* Due to privacy and communication concerns, data cannot be directly shared between client devices and between clients and the central server.

In the railway system, locations of assets are dispersed and there is a considerable distance between devices. Normally, real-time operational data of railway assets is transmitted wirelessly to a central server. Problems of imperfect data transmission including information delay and packet loss occur in the railway system easily. In the existing FL framworks, the central model cannot address those problems. Problems in FL-based fault diagnosis of railway assets are summarized as follows.

1) *Efficient handling of information delay:* In the railway system, the signal propagation time is increased due to

environmental factors such as obstacles. Also, data may undergo multiple paths during propagation, and different parts of the signal may arrive at the receiver at different times due to different path lengths, causing signal delay and distortion. For existing FL frameworks, the fusion algorithm struggles to handle the delays in transmitting data between edge devices and the central server. This delay impacts the overall FL performance negatively, hindering timely decision-making and accurate model updates. Hence, information delay brings the challenge for real-time fault diagnosis with good performance.

2) *Mitigating packet loss impact:* In the railway system, there are numerous sources of interference that may lead to signal attenuation, distortion, or even complete loss. In addition, transmission network congestion may occur if there are a large number of communication requests. Packet loss is a frequent occurrence in wireless communication, especially in scenarios with unstable network conditions. The inability of the central fusion algorithm to handle packet loss effectively results in incomplete or corrupted data, leading to suboptimal model aggregation and compromised learning accuracy. Hence, the following matter has become urgent, i.e., how to obtain high accuracy fault diagnosis result under the condition of packet loss.

Above problems result in inaccuracies and inefficiencies of the existing FL frameworks. In this work, a novel FL-based fault diagnosis of railway point machines is proposed to address these shortcomings.

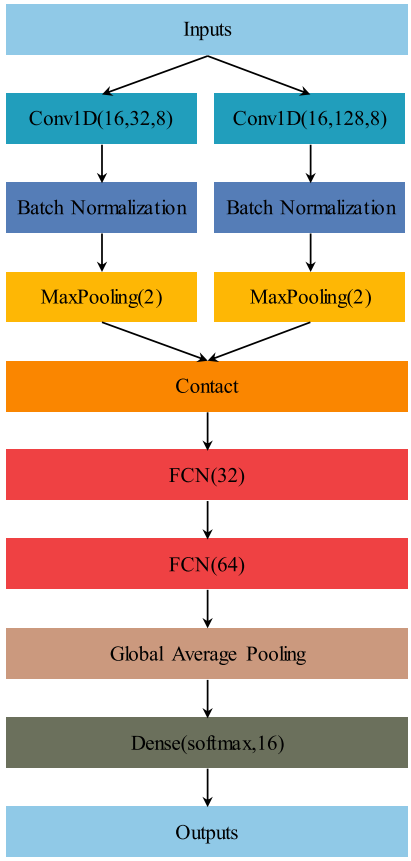

Fig. 2. Structure of DS-FCN.

III. Methodology

A. Double Scale Fully Convolutional Network

The dual-branch network has higher accuracy than the single and multibranch ones [14]. Hence, a DS-FCN is proposed as the global model, as shown in Fig. 2. This model uses two branch structures and employs wide convolutional kernels in the first convolutional layer, following the previous design. The first convolutional kernel extracts features from a larger receptive field and utilizes kernels of varying widths through the two branches to extract features at different scales.

Fig. 3 presents the FCN block. In contrast to the conventional CNN design, it eliminates the intermediate pooling layers positioned between convolutional layers. This modification mitigates the risk of diminishing small-scale features due to maximum pooling and curtails the feature reduction stemming from average pooling. In addition, the dense layers in CNNs have been reduced to encompass solely the softmax output layer, leading to a substantial reduction in trainable parameters. Specifically, the number of trainable parameters has decreased significantly from 38 832 in the DS-WCNN [14] to 28 848.

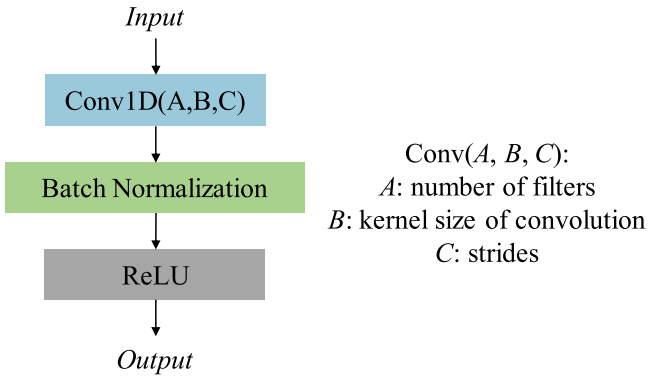

Fig. 3. Structure of FCN block.

B. Asynchronous Federated Network

Assuming that the network model parameters are denoted as $x = [W^T, b^T]^T$, where W and b are the weight and bias of the neurons, respectively. Specifically, for a convolutional layer with i convolutional kernels, x contains i weight matrices and i bias vectors. Since the SKF algorithm is fused based on the same layer of all client parameters, the trainable parameters of various trainable layers can be uniformly represented by x. Typical synchronous aggregation algorithms like FedAvg fuse parameters according to statistical calculations after receiving from all clients.

The Kalman filtering (KF) serves as the fundamental algorithm responsible for estimating global parameters, as opposed to statistical calculations among all clients. In the context of KF, parameters received from the i-th client are treated as the measured values in the ith period of the system. The state model

is implemented as random walk as

$$x(i) = A(i)x(i-1) + \omega_s(i), \tag{1}$$

$$z(i) = H(i)x(i) + \omega_m(i) \tag{2}$$

where $A(i)$ and $H(i)$ are the state transition matrix and observation matrix, respectively. For random walk model $A(i)$ and $H(i)$ can be set as I. $\omega_s(i)$ and $\omega_m(i)$ are Gaussian white noise obeying zero mean. Hence, the prediction-based aggregation can be summarized as

$$\hat{x}(i \mid i-1) = A(i)\hat{x}(i-1), \hat{x}(0) = x(0) \tag{3}$$

$$P(i \mid i-1) = A(i)P(i-1)A^T(i) + Q, P(0) = I \tag{4}$$

where $P(i \mid i-1)$ is the covariance of prior estimation and Q is prediction covariance under Gaussian white noise.

Then, the update function is

$$K(i) = \frac{P(i \mid i-1)H^T(i)}{H(i)P(i \mid i-1)H^T(i) + R} \tag{5}$$

in which $K(i)$ is the Kalman gain for client i and R is the measurement covariance.

After aggregation from client 0 to client i, the global parameters is the update of the period i as

$$\hat{x}(i \mid i) = \hat{x}(i \mid i-1) + K(i)(z(i) - H(i)\hat{x}(i \mid i-1)), \tag{6}$$

$$P(i) = (I - K(i)H(i))P(i \mid i-1). \tag{7}$$

KF establishes estimation for all client parameters received in each federated round. However, it overlooks the interdependencies between different rounds and can be negatively impacted by the uneven distribution of training data. Furthermore, the quality of estimation tends to degrade when some parameters are lost due to packet loss.

SKF builds upon the filtering estimation framework of KF and continues the random walk model. It enhances this process by increasing the number of measurements associated with each state. It treats the model parameter of the ith client in the kth SAFL round as the ith measurement in the kth period, which means prediction of the ith client can be formed through the update of the $(i-1)$th client as

$$\hat{x}_{(i)}(k) = SKF(\hat{x}_{(i-1)}(k), z_i(k)), \tag{8}$$

$$\begin{aligned}
\hat{x}_{(i)}(k \mid k-1) &= \hat{x}_{(i-1)}(k \mid k-1), \\
P_{(i)}(k \mid k-1) &= P_{(i-1)}(k \mid k), \\
\hat{x}_{(0)}(k \mid k) &= \hat{x}(k \mid k-1), \\
P_{(0)}(k \mid k) &= P(k \mid k-1)
\end{aligned} \tag{9}$$

where $\hat{x}_{(i)}(k \mid k-1)$ represents the current estimate for client i, and $P_{(i)}(k \mid k-1)$ shows the covariance of estimation, whereas $\hat{x}_{(0)}(k \mid k)$ serves as the initial global estimate.

C. Time Cycle-Based SAFL

Fig. 1 demonstrates that delays and packet losses significantly impact the time consumption of typical synchronous FL. This is due to the server spending time waiting for all packets to arrive before performing aggregation computations. Hence, it is essential to highlight that synchronous FL typically demands significant robust server-client communication performance and local computing power.

SAFL based on a time cycle mechanism is introduced to terminate a SAFL round once a predefined time limit is reached. This approach is especially valuable in mitigating prolonged waiting periods for all clients, particularly when dealing with poor communication conditions. The SAFL aggregation begins when receives the first parameters. At the kth SAFL round, for each received parameters i, the ith filter is established to iteratively enhance the estimate of the global model parameters. The prediction of $\hat{x}_{(i)}(k \mid k-1)$ and $P_{(i)}(i \mid i-1)$ is calculated according to (3) and (4) as

$$\hat{x}_{(i)}(k \mid k-1) = A_{(i)}(k)\hat{x}_{(i)}(k-1), \tag{10}$$

$$P_{(i)}(i \mid i-1) = A_{(i)}(k)P_{(i)}(k-1)A^T_{(i)}(k) + Q_{(i)} \tag{11}$$

where $\hat{x}_{(i)}(k-1)$ and $P_{(i)}(k-1)$ denotes the latest SKF aggregation result and the covariance in epoch i, respectively.

In FL, the loss of data packets from a certain client can compromise its contribution to the updated global model. If the fusion of parameter packets is reduced in a round due to packet loss, the model parameters may be disproportionately affected, leading to adverse effects on the overall fusion. Hence, it is a problem for obtaining a fair and accurate global fusion when the data packet loss occurs.

To solve the above problem, the Kalman gain plays a crucial role. Acting as a corrective measure, the Kalman gain dynamically adjusts the influence of measurements on system state estimates. When packet loss occurrence causing obstacles to parameter fusion, the Kalman gain prevents negative influence on specific model parameters. By providing a mechanism to handle missing or delayed updates, it ensures a fairer and more accurate global fusion in FL. The Kalman gain $K_{(i)}(k)$ is defined as

$$\begin{aligned}
K_{(i)}(k) = {} & P_{(i)}(k \mid k-1)H^T_{(i)}(k) \\
& \times \left[H_{(i)}(k)P_{(i)}(k \mid k-1)H^T_{(i)}(k) + R_{(i)}(k)\right]^{-1}.
\end{aligned} \tag{12}$$

The covariance matrix of filter state estimation error $P_{(i)}(k+1 \mid k+1)$ is subsequently given by

$$P_{(i)}(k \mid k) = \left[I - K_{(i)}(k)H_{(i)}(k)\right] P_{(i)}(k \mid k-1). \tag{13}$$

According to (9), the update equation for the filter of ith parameters is given by

$$\begin{aligned}
\hat{x}_{(i)}(k \mid k) &= \hat{x}_{(i)}(k \mid k-1) + K_{(i)}(k)\tilde{z}_{(i)}(k \mid k-1) \\
&= \hat{x}_{(i-1)}(k \mid k) + K_{(i)}(k)\tilde{z}_{(i)}(k \mid k-1)
\end{aligned} \tag{14}$$

where the error $\tilde{z}_{(i)}(k \mid k-1)$ is defined by

$$\tilde{z}_{(i)}(k \mid k-1) = z_{(i)}(k) - H_{(i)}(k)\hat{x}_{(i)}(k \mid k-1). \tag{15}$$

As the process unfolds, sequentially filtering from parameter packages 1 through N, the SKF methodology efficiently aggregates the parameter estimates. The final estimate for the global model parameters at time $t+T$ is derived from parameters N as

$$\hat{x}(k \mid k) := \hat{x}_{(N)}(k \mid k). \tag{16}$$

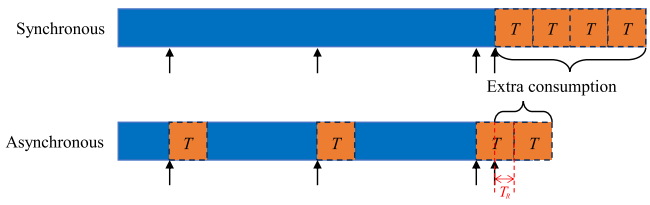

Fig. 4. SAFL integrates the computation time of the server into delay.

The SKF design, which leverages the input from multiple clients, results in a significantly improved estimation of the global model parameters.

In scenarios with significant delays, SAFL utilizes waiting times for subsequent updates, enabling a continuous aggregation process. In contrast, synchronous federated learning requires waiting for all updates to be received before initiating global aggregation. Therefore, in situations with high communication delays, as shown in the Fig. 4, SAFL demonstrates greater flexibility and efficiency. This is notably reflected in the fact that, upon the arrival of the final parameter update, synchronous FL requires an additional time of $(n \times T)$ for the aggregation of n packages, where T denotes the time required for the final update aggregation. While asynchronous FL incurs a time of $(T_R + T)$, where T_R represents the time waiting for the final round of fusion.

D. SAFL Framework-Based Fault Diagnosis for RPMs

The proposed SAFL framwork is shown in Fig. 5. RPMs are denoted as clients and each of them is measured by acceleration sensors continuously. After a fault occurs, the collected vibration data will be labeled and added to the dataset used for training. The SAFL commences when the server dispatches model parameters to all clients. After receiving the global parameters, the client integrates them into its local deep learning model and uses gradient descent to train on the updated training dataset. Following this training, client i forwards the parameters $z_{(i)}(k)$ back to the server.

The server is responsible for continuously receiving and consolidating model parameters from all clients throughout the SAFL period. In SAFL, parameter fusion occurs in the order they are received, without distinguishing individual clients. It starts with the parameters from the first client that arrives and continues until the end of the SAFL cycle. The end of an ASFL cycle is determined by two factors: 1) receiving all clients; or 2) reaching a predetermined arrival time threshold. Due to potential communication pressures or weak signal connections during transmission, significant delays and packet loss may occur. It is impractical for the server to indefinitely await responses from individual clients without constraints. Hence, the time threshold is established as the maximum waiting duration for an ASFL cycle, grounded in practical considerations. The threshold's value is selected by considering factors such as the training duration of each client and the time required for server-side fusion, tailored to real-world application scenarios.

To begin, the prediction of the state x adheres to (10). Subsequently, the sequential Kalman gain is computed as per (12), wherein $P_{(i)}(k \mid k-1)$ is determined using (11). The posterior covariance matrix $P_{(i)}(k \mid k)$ is then generated according to (13).

The update process, transitioning from the $(i-1)$th parameter to the ith parameter, is carried out in accordance with (14) and (15), which are derived from (9). Following the aggregation of all received parameters, the final global model's parameters for a single SAFL period, aggregated a total of N times, are predicted using (16).

Totally speaking, the steps of SAFL are summarized as follows.

1) The global model DSFCN illustrated in Section III-A and the initialized model parameters are created and the model structure without parameters is send to all clients.
2) The server transmits the model parameters to all clients. Clients receive and load these parameters into their local models and proceed to train these models using their respective datasets.
3) The server continually collects and fuses parameters from clients using the SKF shown in Section III-C until the SAFL round is completed.
4) With the start of a new SAFL round, return to Step 2. During this process, clients detect and identify fault types using the most recent model parameters.

IV. Description of RPM Vibration Signals

ZDJ9 RPMs are widely used in high-speed rail and other urban rail transit systems, the structure of ZDJ9 is shown in Fig. 6. When receiving a switching command, the motor in ZDJ9 will engage with the retarder for enhancing torque and transmitting force to the ball screw via a frictional clutch [14]. This conversion of electrical energy facilitated linear motion of the pushing sleeve. Subsequently, the pushing and pulling actions were initiated by the throw rod in relation to the pushing sleeve [12]. Upon detection of movement cessation by the indication rod, the switch circuit controller will deactivate the motor circuit and establish connection with the indication circuit [27].

Faults normally occur in RPM's mechanical and electrical systems. RPM's faults result in variations in switch resistance during the transmission process, and then affecting the speed of the motor. Hence, vibration signals of RPMs have different frequencies and amplitudes under healthy and faulty conditions [28]. Hence, RPM faults can be diagnosed by analyzing vibration signals collected from the motor housing of ZDJ9. In this work, signals with mechanical faults under push-out and pull-in conditions are used to verify the effectiveness of the proposed method. Sixteen scenarios are considered in the experiment section as shown in Table I.

In Table I, the normal movement of RPMs is that the guiding direction of the track is shifted from its typical orientation to a temporary one, facilitating the redirection of trains onto sidings, branch lines, or during track maintenance activities. Once the guiding process is completed, the reverse movement realigns the guiding direction back to its standard direction, enabling trains to resume their usual operational direction [29]. Underdriving (Type a and A) typically occurs due to excessive lubrication of

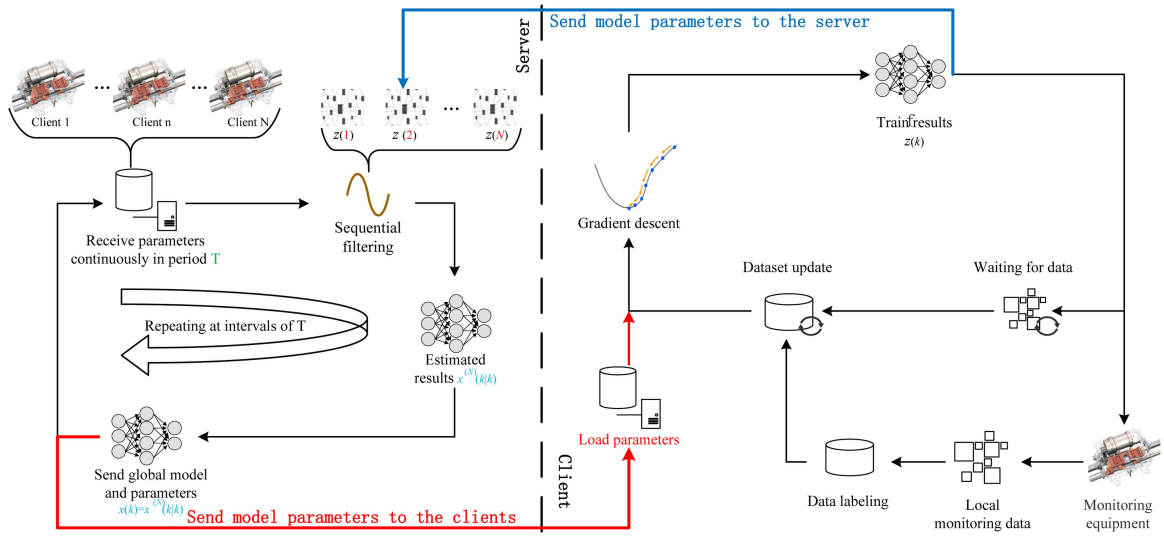

Fig. 5. Framework of the SAFL.

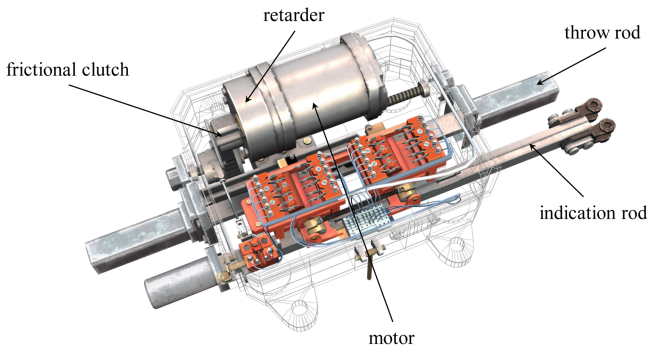

Fig. 6. Structure of ZJD9 RPM.

TABLE I
CONDITIONS OF ZDJ9 RPM

Description	Normal	Reverse
Underdriving, 3kN	a	A
Normal, 4kN	b	B
Overdriving, 5kN	c	C
Overdriving, 6kN	d	D
Sudden indication loss after approaching movement	e	E
Overdriving, 8kN	f	F
No load	g	G
Unlocking failure	h	H

the switch plate, resulting in insufficient output under load. The reasonable output of ZDJ9 is 4 kN (Type b and B). Overdriving at 5 kN (Type c and B) and 6 kN (Type d and D) is attributed to varying degrees of lubricating oil deficiency in the switch plate, with minimal differences in waveform, confirming the model's resolution capability. Sudden indication loss after approaching movement (Type e and E) is caused by the breakage of the indication rod. Overdriving at 8 kN (Type f and F) is commonly caused by obstructions such as gravel. The throw rod breakage leads to the RPM losing load (Type g and G). Unlocking failure (Type h and H) results from severe jamming preventing unlocking. Eight vibration signals with different working conditions during the reverse operation mode are shown in Fig. 7.

V. EXPERIMENT

A. Experiment Setup

For each operating condition shown in Table I, 60 pieces of data were collected, totaling 960 pieces. The ZDJ9 RPM underwent approximately 8 s of operation in each cycle, with a maximum duration of 10 s. To ensure consistent data vector lengths of 10 s (5120 values), the collected raw data underwent necessary trimming and zero-padding. In alignment with the softmax layer's production of a probability distribution, the data labels were similarly represented as probability distributions. Consequently, one-hot encoding is applied to labeling. Data were shuffled and partitioned into the training and testing datasets at the ratio of 8:2.

Within this section, there are three distinct experiments to demonstrate the efficacy of our FCN model, SKF algorithm, and the asynchronous FL framework structure, respectively. The conducted experiments were executed on Intel Corei7-11700 K CPUs (3.6 GHz, 32 GB RAM), supplemented by an NVIDIA GeForce GTX 1080 Ti (CUDA version 10.1). Five clients were simulated on a 64-bit Windows 10 operating system, utilizing Python 3.7 (TensorFlow version 2.3.0). All reported experimental results in this study were obtained by averaging over 30 statistically independent realizations.

B. Global Model Experiment

To test the proposed global model, i.e., DS-FCN, experiments were implemented by comparing with several conventional machine learning algorithms [30], including support vector machine (SVM), random forest (RF), LeNet, AlexNet, recurrent neural network (RNN), and long short-term memory (LSTM) [31] [32]. In addition, our prior DS-WCNN study

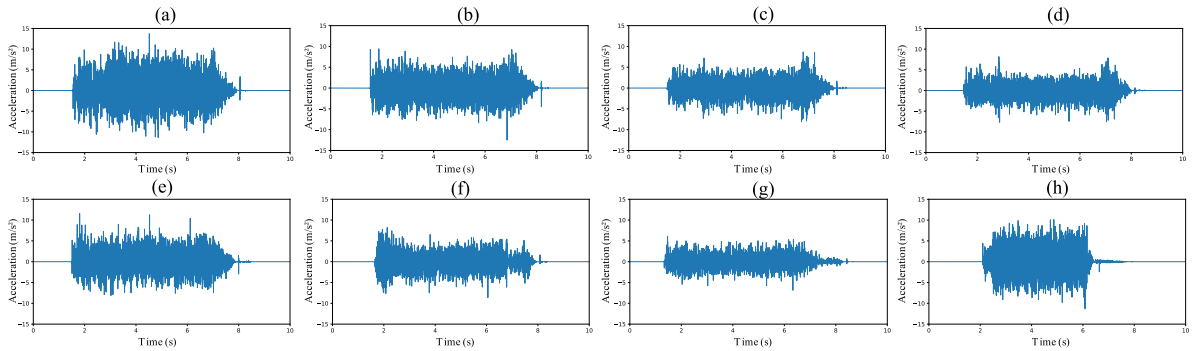

Fig. 7. Waveform of the vibration signal during the reverse operation mode.

TABLE II
ACCURACY OF DIFFERENT METHODS

Algorithm	SVM	RF	LeNet	AlexNet
Accuracy(%)	13.21	44.57	88.57	92.53
Algorithm	RNN	LSTM	DS-WCNN	DS-FCN
Accuracy(%)	49.15	54.22	97.63	97.21

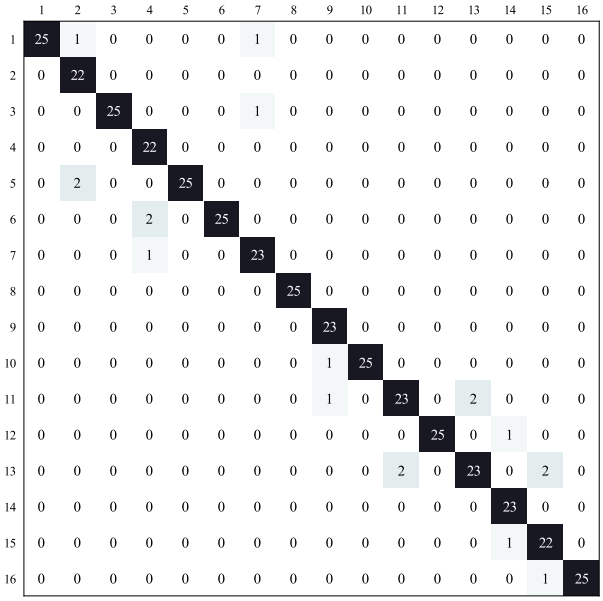

Fig. 8. Confusion matrix on the test set with DS-FCN.

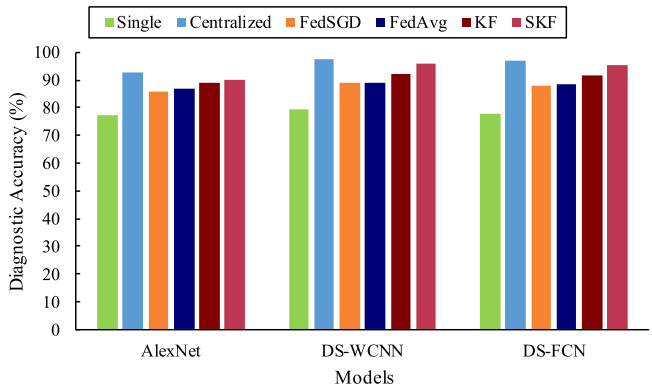

Fig. 9. Diagnosis accuracy of models.

was added for comparison. The accuracy results are detailed in Table II.

Table II shows that DS-FCN has similar accuracy compared to DS-WCNN. However, the DS-FCN only has 28 848 parameters, while the DS-WCNN has 38 832 parameters. The reduction in parameter count helps to minimize communication expenses within the FL framework and reduces the possibilities of congestion and packet loss. As a result, the DS-FCN model whose confusion matrix is shown in Fig. 8 has been designated as the global model for the FL-based RPM fault diagnosis framework.

C. Training Strategy Experiment

To test the proposed training strategies, the experiments are implemented by comparing five different strategies with the proposed method. Fig. 9 shows accuracy of three other models, i.e., AlexNet, DS-WCNN, and DS-FCN with different strategies. It can be seen from Fig. 9 that DS-FCN achieved accuracy levels comparable to DS-WCNN with all six training strategies. In contrast, training on a single device lagged behind in all models because it used limited data, leading to underfitting and overfitting. The centralized training strategy, which used data from all clients for model training, yielded accuracy levels consistent with those presented in Table II.

In the case of FedAvg, the contribution of each device is proportionate to the size of its local dataset. However, the KF-based strategy achieves higher accuracy compared to the baseline strategies by using prior estimation and posterior update. The proposed SKF-based strategy achieved an accuracy of 90.13% on AlexNet, 95.96% on DS-WCNN, and 95.37% on DS-FCN, which significantly outperformed KF. This outstanding performance can be attributed to SKF treating each client's model parameters as individual measurements and employing a sequential aggregation strategy.

The training accuracy curves of different learning strategies are shown in Fig. 10. It can be seen from the figure that the centralized learning approach has the fastest convergence speed primarily by comparing the single strategy and the centralized strategy. The main reason is that the centralized strategy leveraged the dataset containing contributions from all clients, however training the model on a single device alone yielded poor results due to the limited training data. In the figure, both

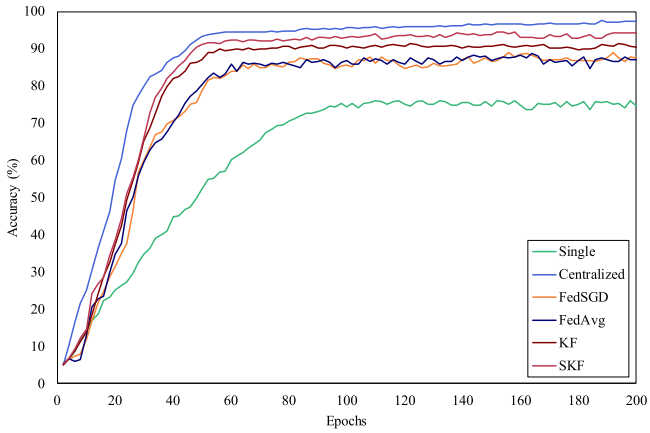

Fig. 10. Training curves of different learning strategies with DS-FCN.

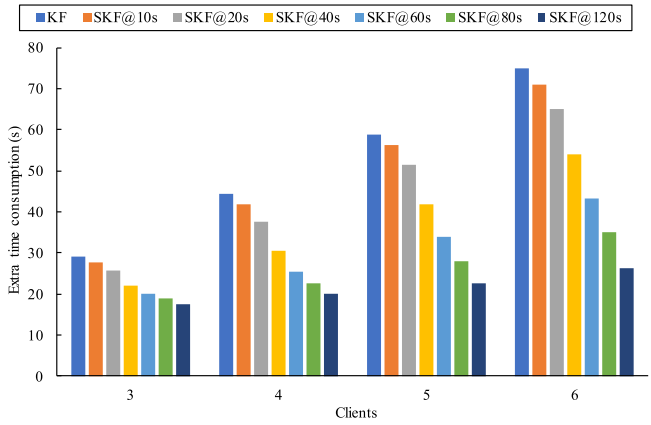

Fig. 11. Extra time consumption for aggregation.

SKF-based and KF-based strategies demonstrated accelerated convergence speeds compared to other strategies because they estimated results based on inputs from individual clients rather than a simple averaging process. It is worth noting that SKF outperformed KF by sequentially aggregating all parameters in a single iteration.

D. Framework Experiment

To better illustrate the superior performance of the SAFL framework under the influence of communication delays between the server and clients, an experiment was set up with delay times uniformly distributed in the range of 0 to $Limit$ seconds. During this experiment, a set of uniformly distributed random numbers $T(C, I)$ ranging from 0 to $Limit$ seconds is generated for each client individually. C represents the number of clients, and I denotes the total epochs of the FL process. After the ith training iteration, client c awaits for $T(c, i)$ seconds before transmitting its model parameters to the server. Subsequently, the server waits until the designated time period elapses before initiating the $(i+1)$th round of FL. In the experiment, $Limit$ was set to different values, specifically 10, 20, 40, 60, 80, and 120 s. The time required for the fusion of each data packet was approximately 15 s. A timer was used to measure the additional time consumed for aggregation, starting from the moment the last parameter was received until the fusion process was completed within the federated cycle.

Fig. 11 shows the extra time consumption for FL frameworks based on KF and SKF in the scenarios of 3, 4, 5, and 6 clients. With increasing communication delays, the SKF-based FL framework demonstrates a significant advantage. The main reason is that the proposed framework can complete parameter fusion while waiting for new parameters simultaneously, whereas the synchronous FL framework based on KF initiates aggregation only after receiving all parameters.

Package loss is another communication error which affects accuracy of FL. In the data packet loss experiment, the data packet loss rate is set to 0, 0.2, 0.4, and 0.6. In this experiment, after completing each round of local training, every client generates a random number. If this number exceeds the experimental packet loss rate R, the client transmits the model parameters

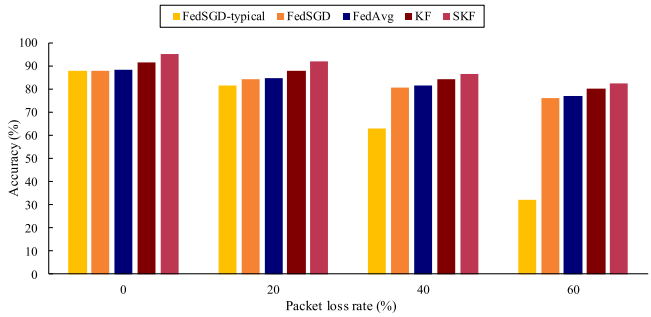

Fig. 12. Diagnosis accuracy under package loss with DS-FCN.

for that round to the server. However, if the generated number is less than R, the client refrains from sending the parameters, thereby simulating packet loss between the server and the client for that particular round. This means that there was a probability of data package loss occurrence, i.e., parameters sent by each client could not be received and fused. The experimental results are shown in the Fig. 12. FedSGD-typical simulates aggregation of parameters only when the server receives all clients, otherwise, it abandons the current round. Compared to other federated aggregation algorithms, the SKF-based FL framework achieves the highest accuracy in all data packet loss scenarios, indicating that SKF is the best aggregation algorithm among various algorithms.

VI. Conclusion

In this work, SAFL framework was proposed for fault diagnosis of RPMs considering the imperfect data transmission problem in this work. In the proposed framework, a DS-FCN was proposed as the global model which reduced the number of parameters by one fourth compared to previous models while maintaining similar levels of accuracy. Less parameters in the global model was helpful for avoiding congestion and package loss in the data transmission. Also, a time cycle mechanism based on SKF was proposed to solve problems of imperfect data transmission. The time cycle-based training strategy enabled removing the prolonged waiting period for all clients when the information delay occured. The sequential Kalman gain was

calculated for preventing negative influence of data package loss. Comparison experiments were implemented and results showed the proposed SAFL framework has greater accuracy than other frameworks at different time delay and packet loss rates.

REFERENCES

[1] Y. Li, F. Liu, S. Wang, and J. Yin, "Multiscale symbolic Lempel–Ziv: An effective feature extraction approach for fault diagnosis of railway vehicle systems," *IEEE Trans. Ind. Inform.*, vol. 17, no. 1, pp. 199–208, Jan. 2021.

[2] A. Nunez, A. Jamshidi, and H. Wang, "Pareto-based maintenance decisions for regional railways with uncertain weld conditions using the hilbert spectrum of axle box acceleration," *IEEE Trans. Ind. Inform.*, vol. 15, no. 3, pp. 1496–1507, Mar. 2019.

[3] M. Karakose and O. Yaman, "Complex fuzzy system based predictive maintenance approach in railways," *IEEE Trans. Ind. Inform.*, vol. 16, no. 9, pp. 6023–6032, Sep. 2020.

[4] Q. Wang, S. Lin, T. Li, and Z. He, "Intelligent proactive maintenance system for high-speed railway traction power supply system," *IEEE Trans. Ind. Inform.*, vol. 16, no. 11, pp. 6729–6739, Nov. 2020.

[5] F. P. G. Márquez, C. Roberts, and A. M. Tobias, "Railway point mechanisms: Condition monitoring and fault detection," *Proc. Inst. Mech. Eng., Part F: J. Rail Rapid Transit*, vol. 224, no. 1, pp. 35–44, 2010.

[6] X. Hu, Y. Cao, Y. Sun, and T. Tang, "Railway automatic switch stationary contacts wear detection under few-shot occasions," *IEEE Trans. Intell. Transp. Syst.*, vol. 23, no. 9, pp. 14893–14907, Sep. 2022.

[7] X. Hu, T. Tang, L. Tan, and H. Zhang, "Fault detection for point machines: A review, challenges, and perspectives," *Actuators*, vol. 12, no. 10, 2023, Art. no. 391.

[8] Z. Feng and M. J. Zuo, "Vibration signal models for fault diagnosis of planetary gearboxes," *J. Sound Vib.*, vol. 331, no. 22, pp. 4919–4939, 2012.

[9] C. Li, R.-V. Sánchez, G. Zurita, M. Cerrada, and D. Cabrera, "Fault diagnosis for rotating machinery using vibration measurement deep statistical feature learning," *Sensors*, vol. 16, no. 6, 2016, Art. no. 895.

[10] V. D. Abhijit, V. Sugumaran, and K. I. Ramachandran, "Fault diagnosis of bearings using vibration signals and wavelets," *Indian J. Sci. Technol.*, vol. 9, no. 33, 2016.

[11] X. Hu, Y. Cao, T. Tang, and Y. Sun, "Data-driven technology of fault diagnosis in railway point machines: Review and challenges," *Transp. Saf. Environ.*, vol. 4, no. 4, 2022, Art. no. tdac036.

[12] Y. Sun, Y. Cao, H. Liu, W. Yang, and S. Su, "Condition monitoring and fault diagnosis strategy of railway point machines using vibration signals," *Transp. Saf. Environ.*, vol. 5, no. 2, 2023, Art. no. tdac048.

[13] X. Wu, W. Yang, and J. Cao, "Fault diagnosis of railway point machines based on wavelet transform and artificial immune algorithm," *Transp. Saf. Environ.*, vol. 5, 2022, Art. no. tdac072.

[14] X. Chen, X. Hu, T. Wen, and Y. Cao, "Vibration signal-based fault diagnosis of railway point machines via double-scale CNN," *Chin. J. Electron.*, vol. 32, no. 5, pp. 972–981, 2023.

[15] Y. Cao, Y. Ji, Y. Sun, and S. Su, "The fault diagnosis of a switch machine based on deep random forest fusion," *IEEE Intell. Transp. Syst. Mag.*, vol. 15, no. 1, pp. 437–452, Jan./Feb. 2023.

[16] T. Li, A. K. Sahu, A. Talwalkar, and V. Smith, "Federated learning: Challenges, methods, and future directions," *IEEE Signal Process. Mag.*, vol. 37, no. 3, pp. 50–60, May 2020.

[17] L. Li, Y. Fan, M. Tse, and K.-Y. Lin, "A review of applications in federated learning," *Comput. Ind. Eng.*, vol. 149, 2020, Art. no. 106854.

[18] S. Banabilah, M. Aloqaily, E. Alsayed, N. Malik, and Y. Jararweh, "Federated learning review: Fundamentals, enabling technologies, and future applications," *Inf. Process. Manage.*, vol. 59, no. 6, 2022, Art. no. 103061.

[19] S. Ek, F. Portet, P. Lalanda, and G. Vega, "Evaluation and comparison of federated learning algorithms for human activity recognition on smartphones," *Pervasive Mobile Comput.*, vol. 87, 2022, Art. no. 101714.

[20] N. Rieke et al., "The future of digital health with federated learning," *NPJ Digit. Med.*, vol. 3, no. 1, 2020, Art. no. 119.

[21] W. Zhang et al., "R ^{2} fed: Resilient reinforcement federated learning for industrial applications," *IEEE Trans. Ind. Inform.*, vol. 19, no. 8, pp. 8829–8840, Aug. 2023.

[22] S. Messaoud, A. Bradai, O. B. Ahmed, P. T. A. Quang, M. Atri, and M. S. Hossain, "Deep federated Q-learning-based network slicing for industrial IoT," *IEEE Trans. Ind. Inform.*, vol. 17, no. 8, pp. 5572–5582, Aug. 2021.

[23] W. Zhang, X. Li, H. Ma, Z. Luo, and X. Li, "Federated learning for machinery fault diagnosis with dynamic validation and self-supervision," *Knowl.-Based Syst.*, vol. 213, 2021, Art. no. 106679.

[24] S. Lu, Z. Gao, Q. Xu, C. Jiang, A. Zhang, and X. Wang, "Class-imbalance privacy-preserving federated learning for decentralized fault diagnosis with biometric authentication," *IEEE Trans. Ind. Inform.*, vol. 18, no. 12, pp. 9101–9111, Dec. 2022.

[25] N. Qin, J. Du, Y. Zhang, D. Huang, and B. Wu, "Fault diagnosis of multi-railway high-speed train bogies by improved federated learning," *IEEE Trans. Veh. Technol.*, vol. 72, no. 6, pp. 7184–7194, Jun. 2023.

[26] X. Ma, C. Wen, and T. Wen, "An asynchronous and real-time update paradigm of federated learning for fault diagnosis," *IEEE Trans. Ind. Inform.*, vol. 17, no. 12, pp. 8531–8540, Dec. 2021.

[27] Y. Cao, Y. Sun, G. Xie, and P. Li, "A sound-based fault diagnosis method for railway point machines based on two-stage feature selection strategy and ensemble classifier," *IEEE Trans. Intell. Transp. Syst.*, vol. 23, no. 8, pp. 12074–12083, Aug. 2022.

[28] X. Hu et al., "Railway switch machine fault diagnosis considering sensor abnormality scenarios," in *Proc. IEEE 26th Int. Conf. Intell. Transp. Syst.*, 2023, pp. 4834–4839.

[29] X. Hu, R. Niu, and T. Tao, "Research on entropy based corrective maintenance difficulty estimation of metro signaling," in *Proc. IEEE Intell. Transp. Syst. Conf.*, 2019, pp. 79–85.

[30] H. Wang, Z. Liu, D. Peng, and M. J. Zuo, "Interpretable convolutional neural network with multilayer wavelet for noise-robust machinery fault diagnosis," *Mech. Syst. Signal Process.*, vol. 195, 2023, Art. no. 110314.

[31] C. He, H. Shi, J. Si, and J. Li, "Physics-informed interpretable wavelet weight initialization and balanced dynamic adaptive threshold for intelligent fault diagnosis of rolling bearings," *J. Manuf. Syst.*, vol. 70, pp. 579–592, 2023.

[32] C. He, X. Huo, C. Zhu, and S. Chen, "Feature selection-based multi-view concentration for multivariate time series classification and its application," *IEEE Sensors J.*, vol. 24, no. 4, pp. 4798–4806, Feb. 2024.

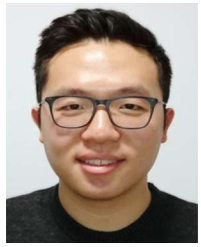

Tao Wen received the B.Eng. degree in computer science from Hangzhou Dianzi University, Hangzhou, China, in 2011, the M.Sc. degree in wireless communication from the University of Bristol, Bristol, U.K., in 2013, and the Ph.D. degree in railway control systems from the Birmingham Centre for Railway Research and Education, University of Birmingham, Birmingham, U.K., in 2018.

He is currently with Beijing Jiaotong University, Beijing, China. His research interests include train control system optimization, railway conditional monitoring, machine learning, and digital filter research.

Xiaohan Chen received the B.Eng degree in communication engineering, in 2022, from Beijing Jiaotong University, Beijing, China, where he is currently working toward the master's degree in traffic information engineering and control.

His research interests include federated learning and deep learning in railway fault diagnosis.

Dingcheng Zhang received the Ph.D. degree in railway control systems from the Birmingham Centre for Railway Research and Education, University of Birmingham, Birmingham, U.K., in 2020.

He was the Postdoctoral Researcher with the Department of Systems Engineering and Engineering Management, City University of Hong Kong, Kowloon, Hong Kong, in 2021. He is currently an Associate Professor with the School of Mechanical Engineering, Sichuan University, Chengdu, China. His research interests include signal processing and machine learning, fault diagnosis and prognosis, intelligent condition monitoring, and maintenance.

Clive Roberts (Member, IEEE) received the B.Eng. degree from the University of Wales, Cardiff, U.K., in 1996, and the Ph.D. degree from the University of Birmingham, Birmingham, U.K., in 2006.

He is currently a Professor of railway systems with the University of Birmingham, Birmingham, U.K. He is also the Director of the Birmingham Centre for Railway Research and Education, which is the largest railway research group in Europe with over 100 researchers. He works extensively with the railway industry and academia in Britain and overseas. He leads a broad portfolio of research aimed at improving the performance of railway systems, including leading a strategic partnership in the area of data integration with Network Rail. His main research interests include railway traffic management, condition monitoring, energy simulation, and system integration.

Baigen Cai (Senior Member, IEEE) received the B.S., M.S., and Ph.D. degrees in traffic information engineering and control from Beijing Jiaotong University, Beijing, China, in 1987, 1990, and 2010, respectively.

In 2016, he was the Dean with the School of Computer and Information Technology, Beijing Jiaotong University, where he is currently the Dean with the School of Automation and Intelligence. His research interests include train control systems, ITS, and GNSS navigation.